

## **Numerical simulation of nonlinear ultrasonic waves for bi-material interface evaluation**

\*Sohichi Hirose<sup>1)</sup>, Taizo Maruyama<sup>2)</sup> and Takahiro Saitoh<sup>3)</sup>

<sup>1), 2)</sup> *Department of Mechanical and Environmental Informatics,  
Tokyo Institute of Technology, Tokyo 152-8552, Japan*

<sup>3)</sup> *Division of Environmental Engineering Science, Gunma University,  
Gunma 376-8515, Japan*

<sup>1)</sup> shirose@cv.titech.ac.jp

### **ABSTRACT**

Boundary integral equations are formulated to investigate nonlinear waves generated by a debonding interface of bi-material subjected to an incident plane wave, and the IRK (Implicit Runge-Kutta method) based CQ-BEM (Convolution Quadrature-Boundary Element Method) is implemented in the numerical simulation. The interface conditions for a debonding area, consisting of three phases of separation, stick and slip, are developed for the simulation of nonlinear ultrasonic waves. Numerical results are obtained and discussed for normal and oblique incidences of plane P waves into the nonlinear interface.

### **1. INTRODUCTION**

Nonlinear ultrasonic nondestructive testing has been developed over the last decade (Solodov *et al.* 2011), since nonlinear waves are generated by material nonlinearity and nonlinear boundary conditions and are very sensitive to degradation of material properties at very early stage. However, the mechanism of generation of nonlinear waves is not yet understood very well from the theoretical and/or numerical point of view.

So far, two dimensional simulations on nonlinear ultrasonic waves have been carried out (Hirose 1994, Saitoh *et al.* 2011). However, no three dimensional analysis has been done. It is, therefore, demanded to conduct numerical simulations with three dimensional realistic models. In this paper, three dimensional boundary integral equations are formulated for a penny-shaped interface crack with nonlinear boundary conditions in bi-material half spaces. The integral equations are discretized using the IRK based CQ-BEM and numerically solved to investigate the nonlinearity involved in ultrasonic waves scattered by the nonlinear interface crack.

---

<sup>1)</sup> Professor

<sup>2)</sup> Graduate Student

<sup>3)</sup> Associate Professor

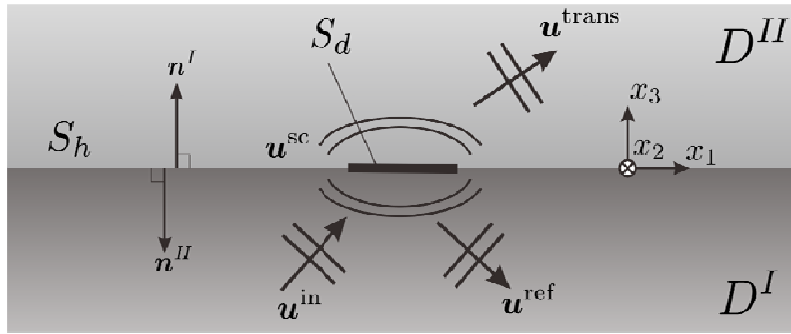


Fig. 1 Model for numerical simulation.

## 2. Formulation of boundary integral equations

The model of a bi-material, consisting of two semi-infinite domains  $D^I$  and  $D^{II}$ , is shown in Fig.1.  $S_h$  and  $S_d$  represent the bonding and debonding areas, respectively, of the bi-material interface. Assuming that an incident plane wave is given in  $D^I$ , we may formulate time-domain boundary integral equations, in which reflected and transmitted waves are unknown values. However, the time-domain boundary integral equations for the bi-material have the following disadvantages;

- 1) For normal incidence of a plane wave, reflection and transmission occur at all points on the interface from the initial step in time. Due to this fact, truncation errors can be introduced at the edge element, where the infinite interface is truncated in numerical analysis.
- 2) For oblique incidence, initial conditions that are given by zero displacement and velocity for unknown reflected and transmitted waves at all points in the domains, cannot be satisfied unless an infinite interface is taken into account in the numerical analysis.

Therefore, in this paper, the integral formulation in which unknown variables are only scattered waves from the debonding area, is proposed in order to overcome these difficulties. If the flat interface of infinite extent is perfectly bonded and is subjected to a plane wave incidence, it is easy to calculate analytically the "free field  $\mathbf{u}^{\text{free}}$ ", defined as the summation of the incident wave  $\mathbf{u}^{\text{in};I}$  and the reflected wave  $\mathbf{u}^{\text{ref};I}$  in  $D^I$ , and the transmitted wave field  $\mathbf{u}^{\text{trans};II}$  in  $D^{II}$  as follows;

$$\mathbf{u}^{\text{free};I} = \mathbf{u}^{\text{in};I} + \mathbf{u}^{\text{ref};I} \quad : D^I, \quad (1)$$

$$\mathbf{u}^{\text{free};II} = \mathbf{u}^{\text{trans};II} \quad : D^{II}. \quad (2)$$

If debonding exists in a local area on the interface, the free field may be disturbed by the wavefield  $\mathbf{u}^{\text{sc}}$  scattered by the debonding, and the total displacement  $\mathbf{u}$  can be expressed by

$$\mathbf{u}^{I \text{ or } II} = \mathbf{u}^{\text{free}; I \text{ or } II} + \mathbf{u}^{\text{sc}; I \text{ or } II} : D^{I \text{ or } II}. \quad (3)$$

Since the scattered wave  $\mathbf{u}^{\text{sc}}$  satisfies the initial condition and the radiation condition, the boundary integral equations for  $\mathbf{u}^{\text{sc}}$  are formulated in a usual manner as follows;

$$\begin{aligned} \mathbf{C}(\mathbf{x})\mathbf{u}^{\text{sc}; I \text{ or } II}(\mathbf{x}, t) = & \int_{S_h+S_d} \mathbf{U}(\mathbf{x}, \mathbf{y}, t) * \mathbf{t}^{\text{sc}; I \text{ or } II}(\mathbf{y}, t) dS_y \\ & - p.v. \int_{S_h+S_d} \mathbf{T}(\mathbf{x}, \mathbf{y}, t) * \mathbf{u}^{\text{sc}; I \text{ or } II}(\mathbf{y}, t) dS_y : D^{I \text{ or } II}, \end{aligned} \quad (4)$$

where  $\mathbf{C}$  is the free term (Brebbia 1984) depending on the boundary shape at  $\mathbf{x}$ ,  $\mathbf{t}$  is the traction force, and  $\mathbf{U}$  and  $\mathbf{T}$  are the fundamental solutions for displacement and traction, respectively. The *p.v.* means the Cauchy's principle integral, and  $*$  means the convolution integral. Substituting eq. (3) into eq. (4), the integral formulation for the bi-material subjected to the incident plane wave can be obtained as follows:

$$\begin{aligned} \mathbf{C}(\mathbf{x})\mathbf{u}^{I \text{ or } II}(\mathbf{x}, t) = & \mathbf{C}(\mathbf{x})\mathbf{u}^{\text{free}; I \text{ or } II}(\mathbf{x}, t) \\ & + \int_{S_h+S_d} \mathbf{U}(\mathbf{x}, \mathbf{y}, t) * \{\mathbf{t}^{I \text{ or } II}(\mathbf{y}, t) - \mathbf{t}^{\text{free}; I \text{ or } II}(\mathbf{y}, t)\} dS_y \\ & - p.v. \int_{S_h+S_d} \mathbf{T}(\mathbf{x}, \mathbf{y}, t) * \{\mathbf{u}^{I \text{ or } II}(\mathbf{y}, t) - \mathbf{u}^{\text{free}; I \text{ or } II}(\mathbf{y}, t)\} dS_y : D^{I \text{ or } II} \end{aligned} \quad (5)$$

Eq. (5) is solved simultaneously using appropriate boundary conditions on the interface  $S_h$  and  $S_d$ . The IRK based CQM is applied to eq.(5) to discretize and calculate the convolution integral stably and accurately in a time-stepping procedure.

### 3. Discretization using IRK based CQM

In solving the boundary integral equations (5) numerically, the convolution integrals are evaluated by the IRK based CQM (Lubich et al. 1993) and the surface integrals over the bonding and debonding interfaces are discretized by constant elements, where the unknown values are assumed to be constant on an element. If the  $m$ -stage Radau IIA method, which is one of IRK methods, is used in the IRK based CQM, and the interface is divided into  $M$  constant elements, the discretized boundary integral equations at the  $n$  step and the  $i$  sub-step in time are shown as:

$$\begin{aligned}
\mathbf{C}(\mathbf{x})\mathbf{u}_\gamma^{I \text{ or } II}((n + c_i)\Delta t) &= \mathbf{C}(\mathbf{x})\mathbf{u}_\gamma^{\text{free}; I \text{ or } II}((n + c_i)\Delta t) \\
&+ \sum_{k=0}^n \sum_{\alpha=1}^M \sum_{j=1}^m [A_{\gamma\alpha}^{ij;n-k} \{ \mathbf{t}_\alpha^{I \text{ or } II}((k + c_j)\Delta t) - \mathbf{t}_\alpha^{\text{free}; I \text{ or } II}((k + c_j)\Delta t) \} \\
&\quad - \mathbf{B}_{\gamma\alpha}^{ij;n-k} \{ \mathbf{u}_\alpha^{I \text{ or } II}((k + c_j)\Delta t) - \mathbf{u}_\alpha^{\text{free}; I \text{ or } II}((k + c_j)\Delta t) \}],
\end{aligned} \tag{6}$$

where,  $\alpha$  and  $\gamma$  are the indexes of constant elements,  $c_i$  are parameters in the IRK method, and  $A_{\gamma\alpha}^{ij;\kappa}$  and  $B_{\gamma\alpha}^{ij;\kappa}$  are time-domain influence functions defined by

$$\mathbf{A}_{\gamma\alpha}^{ij;\kappa} = \frac{\mathcal{R}^{-\kappa}}{L} \sum_{l=0}^{L-1} \left[ \sum_{\beta=1}^m \mathbf{E}_\beta(\zeta_l) \int_{S_\alpha} \widehat{\mathbf{U}}(\mathbf{x}_\gamma, \mathbf{y}, \lambda_\beta^l) dS_y \right] e^{-\frac{2\pi i \kappa l}{L}}, \tag{7}$$

$$\mathbf{B}_{\gamma\alpha}^{ij;\kappa} = \frac{\mathcal{R}^{-\kappa}}{L} \sum_{l=0}^{L-1} \left[ \sum_{\beta=1}^m \mathbf{E}_\beta(\zeta_l) p.v. \int_{S_\alpha} \widehat{\mathbf{T}}(\mathbf{x}_\gamma, \mathbf{y}, \lambda_\beta^l) dS_y \right] e^{-\frac{2\pi i \kappa l}{L}}. \tag{8}$$

where  $\widehat{\mathbf{U}}(\mathbf{x}, \mathbf{y}, s)$  and  $\widehat{\mathbf{T}}(\mathbf{x}, \mathbf{y}, s)$  are the Laplace domain fundamental solutions for displacement and traction, respectively, and  $s$  is the Laplace parameter. In addition,  $\lambda_\beta^l, \mathcal{R}, L, \zeta_l$ , and  $\mathbf{E}_\beta$  are parameters of IRK based CQM (Maruyama et al. 2012). Matrix-vector products on the right side of eq.(6) are effectively calculated by means of the fast multipole method (Saitoh et al. 2010).

#### 4. Interface conditions of bonding and debonding areas

Eq.(6) can be transformed into the system of equations and solved by introducing appropriate conditions on the interface. The interface condition on the bonding area is the continuity of displacement and stress as follows;

$$\mathbf{u}^I = \mathbf{u}^{II}, \quad \mathbf{t}^I = -\mathbf{t}^{II}. \tag{9}$$

For the debonding area, three types of interface conditions are considered as shown in Fig.2 (Hirose 1994). In Fig.2, “separation” means that two surfaces of upper and lower materials are separated with no traction, while “stick” and “slip” are contact conditions under compressive normal stress state. For the “stick” condition, the surfaces of two materials move with no relative velocity. On the other hand, the “slip” condition allows a relative tangential movement with dynamic friction force.

##### 4.1 Separation condition

The “separation” means non-contact condition, and the boundary conditions are given as stress free conditions.

$$\mathbf{t}^I = \mathbf{t}^{II} = \mathbf{0} \quad (10)$$

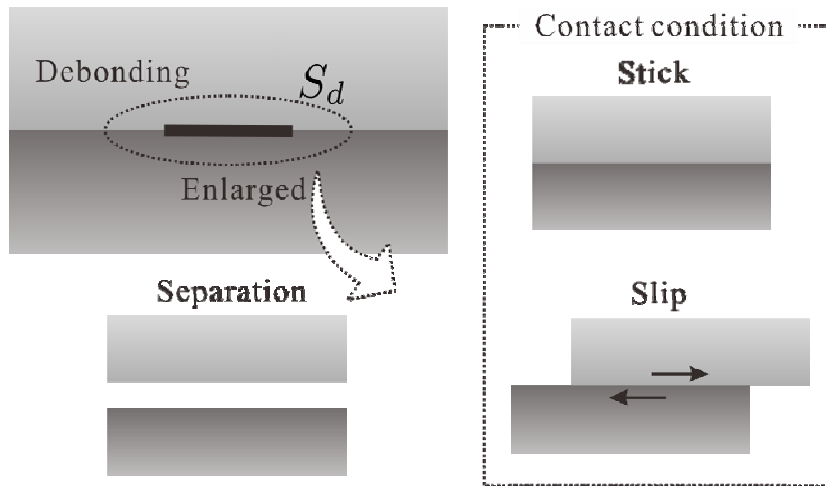


Fig. 2 Debonding conditions on bi-material interface.

#### 4.2 Stick condition

The “stick” condition means contact and non-slip state. Thus, the normal displacement and stresses are continuous across the interface. Also, this condition allows no relative tangential velocities, keeping the discontinuity of tangential displacements statically constant on the interface. Thus, the “stick” conditions are described as;

$$u_3^I = u_3^{II} + g, \quad \mathbf{t}^I = -\mathbf{t}^{II}, \quad \mathbf{v}_s = \mathbf{0}, \quad (11)$$

where  $\mathbf{v}_s$  is the relative velocity between upper and lower surfaces, defined by  $\mathbf{v}_s = \dot{\mathbf{u}}_s^{II} - \dot{\mathbf{u}}_s^I$  and the subscript  $s$  means the tangential component and  $g$  is the initial opening displacement on the debonding area.

#### 4.3 Slip condition

The “slip” condition allows relative slides with friction in tangential directions on the interface. Then, the absolute value of tangential traction can be calculated by use of the Coulomb friction rule, i.e., the normal traction force multiplied by the coefficient of kinematic friction  $\mu_d$ . Then the conditions of “slip” are shown as;

$$u_3^I = u_3^{II} + g, \quad t_3^I = -t_3^{II}, \quad \mathbf{t}_s^I = -\mathbf{t}_s^{II} = \frac{\mathbf{v}_s}{|\mathbf{v}_s|} \mu_d (-t_3^I). \quad (12)$$

## 5. Numerical procedure

The numerical algorithm is shown in Fig.3. At a time step in the IRK method, the discretized equation (6) is solved assuming that the interface conditions on each element are the same as those in the previous time step. If the additional constraint conditions enclosed by the double rhombuses in Fig.3 are not satisfied by the obtained

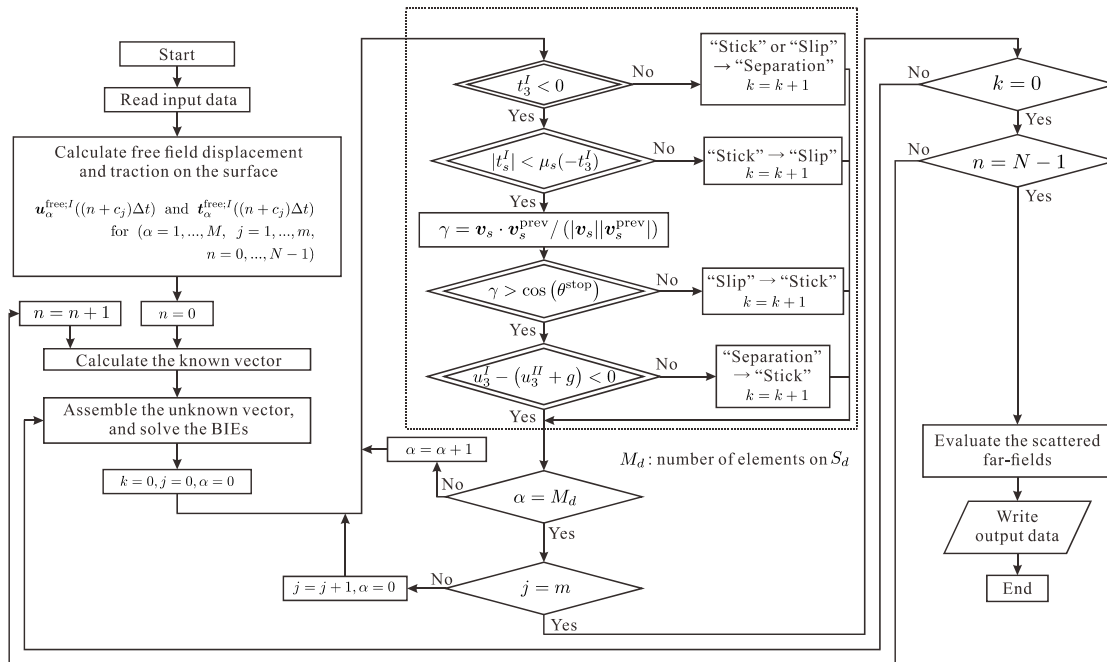


Fig. 3 Numerical algorithm

solutions, the interface condition on the element, which is one of separation, stick and slip, is changed to another condition and then the system of equations is assembled and solved again. After conducting the iterative calculations, if both the boundary conditions and the additional constraint conditions on all elements are satisfied, the time step proceeds to the next one.

Some remarks concerning the numerical calculations are given below. At the initial time step, the interface condition of separation is given on all elements on the debonding area assuming that the interface has an initial opening displacement  $g$  before the wave incidence. There are two options for the phase shift from "separation" to one of two contact conditions, i.e., slip and stick. In the present study, the priority is given to the change from separation to stick, if  $u_3^I - (u_3^{II} + g) < 0$  for the separation condition is violated on the element. In numerical calculations, it is difficult to achieve

the condition  $v_s = \mathbf{0}$  exactly in the transition from stick to slip. Therefore we set  $v_s = \mathbf{0}$  if the following condition is not satisfied:

$$\gamma > \cos(\theta^{\text{stop}}) \quad (13)$$

where  $\gamma = v_s \cdot v_s^{\text{prev}} / (|v_s| |v_s^{\text{prev}}|)$  and  $v_s^{\text{prev}}$  is the relative horizontal displacement velocity at the previous time step. Eq.(13) means that the transition from slip to stick occurs when there is a big change in the slip direction. In this study,  $\theta^{\text{stop}}$  is given by 170 degrees.

## 6. Numerical examples

We present two numerical examples for nonlinear ultrasonic wave problems of bi-material interface subjected to (1) normal incidence of a P wave and (2) oblique incidence of a P wave. The debonding area is a pennyshaped interface crack with radius 0.5mm. Assume that the material constants for bi-material are given in Table.1, and the coefficients of static and kinematic friction are given by  $\mu_s = 0.61$  and  $\mu_d = 0.47$ , respectively. The initial opening displacement  $g$  is given by  $g = 5\text{nm}$ , and the incident wave is a sinusoidal plane wave with three cycles and 10nm amplitude.

Table. 1 Material constants

	$c_L$ [mm/ $\mu$ s]	$c_T$ [mm/ $\mu$ s]	$\rho$ [ $\mu$ g/mm <sup>3</sup> ]
$D^I$ (steel)	5.80	3.10	7.69
$D^{II}$ (aluminum)	6.40	3.04	2.70

### 6.1 Normal incidence of a P wave

Firstly the numerical results for normal incidence are shown. In Fig. 4, the vertical displacements (left column) and the crack opening displacements (right column) at the center points on the upper and lower debonding surfaces are demonstrated as a function of time for the sinusoidal incident P waves with 4, 6, and 8 MHz frequencies. In the case of 4MHz, the behaviors of displacements are almost periodic, whereas in the cases of 6MHz and 8MHz, the waveforms are irregularly disordered due to the interaction between upper and lower surfaces.

In Fig. 5, the vertical displacements of total wave fields (left column) and the Fourier spectra (right column) at the internal point located 0.1mm above the center of the debonding area are shown for the sinusoidal incident P waves with 4, 6, and 8 MHz frequencies, compared with the results for free fields that are the wave fields in a bi-material without debonding. In the case of 4MHz, the time variation of vertical displacement shows the nearly half-wave rectification due to the contact of interfaces, and the Fourier spectrum shows the second and higher harmonics as well as relatively large sub-harmonics. In the cases of 6 MHz and 8 MHz, the displacements show positive and negative oscillations in time and second harmonics in the Fourier spectra. However, sub-harmonics are not so enhanced as in the case of 4MHz.

From these results, it can be seen that nonlinear ultrasonic waves like higher harmonics and sub-harmonics are generated, largely depending on the contact conditions on the interface.

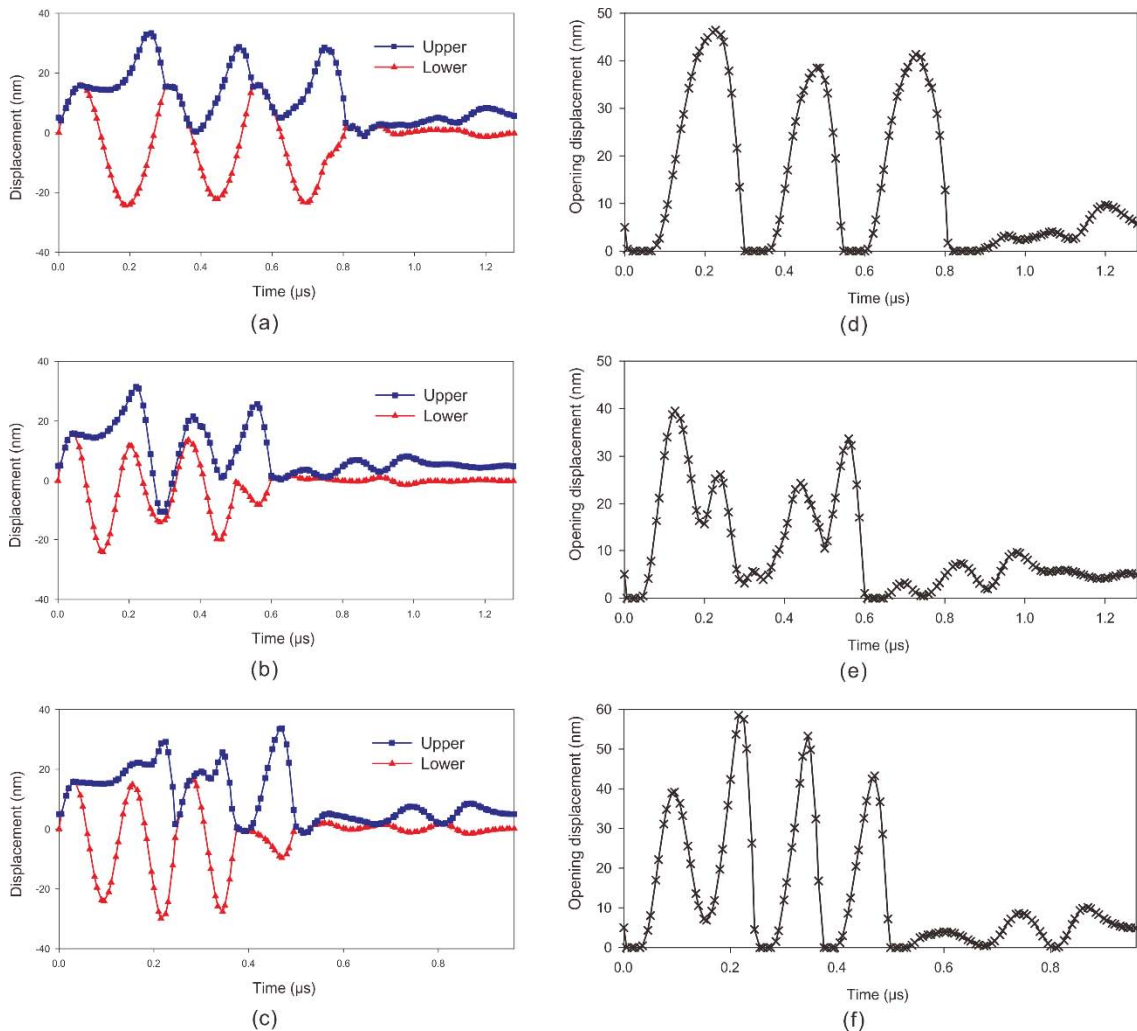


Fig. 4 Time variations of vertical displacements at the center points on upper and lower debonding surfaces (left column) and crack opening displacements at the center (right column) in the cases of normal incidence of sinusoidal P waves with 4MHz (top), 6MHz (middle) and 8MHz (bottom) frequencies.

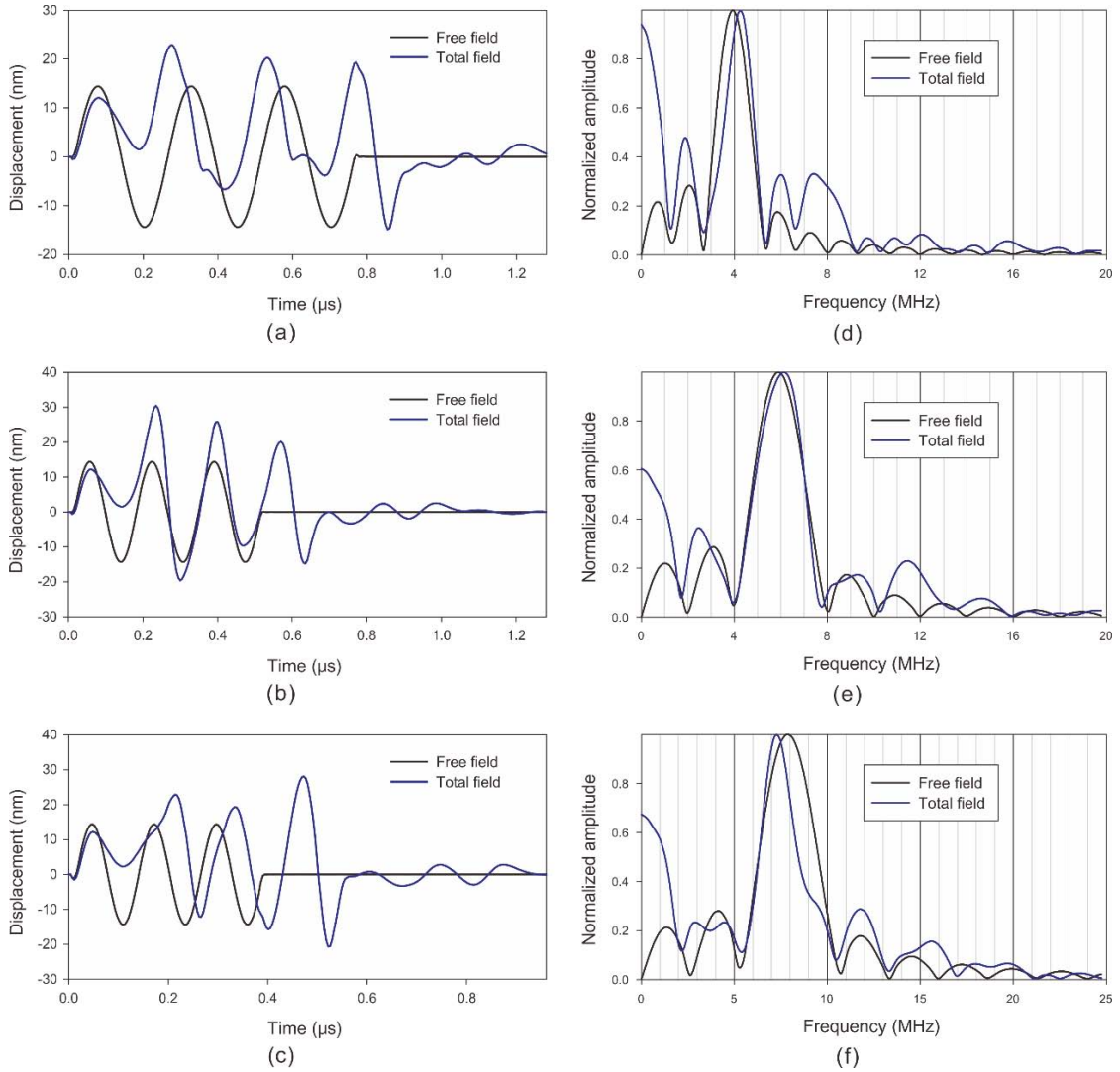


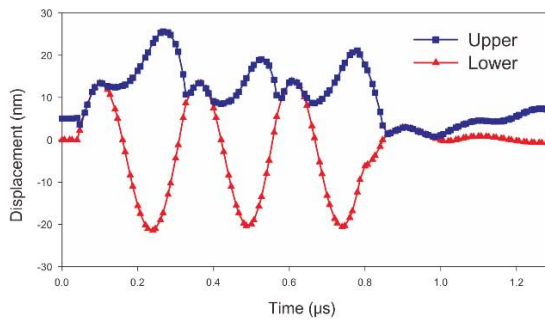
Fig. 5 Vertical displacements as a function of time (left column) and Fourier spectra (right column) at the point 0.1mm above the center on debonding surfaces in the cases of normal incidence of sinusoidal P waves with 4MHz (top), 6MHz (middle) and 8MHz (bottom) frequencies.

### 6.2 Oblique incidence of a P wave

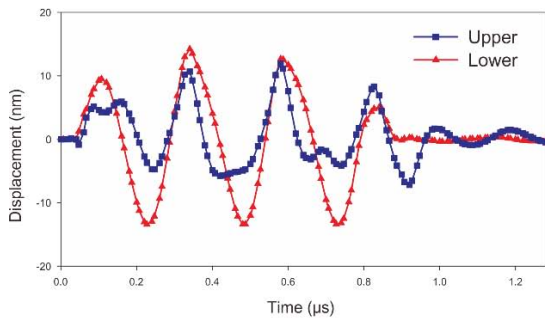
In order to observe the influence of incident angle, we consider the oblique incidence of a 4MHz sinusoidal P wave. The incident angle is 30 degrees in  $x_1$ - $x_3$  plain. Figs. 6 (a) and (b) show time variations of vertical and horizontal displacement components, respectively, at the center points on the upper and lower debonding surfaces. Both results give nearly periodic motions. Vertical and horizontal components of crack opening displacements are shown in Fig. 6 (c). The horizontal component changes in a very nonlinear way during contact phase, because of the difference between the static and dynamic friction coefficients. Figs. 7 (a) and (b) show the amplitudes of vertical and horizontal displacements, respectively, as a function of time at the internal point, 0.1mm above the center of the debonding area. It can be seen that the vertical component demonstrates large positive bias, and the horizontal component shows obviously nonlinear behaviors, i.e., different waveforms on positive and negative sides as seen in Fig. 7 (b). Fourier spectra of these waveforms are shown in Fig. 7 (c). We can see that higher harmonic waves are very clearly found in the spectrum of horizontal displacement at 8, 12, and 16MHz. Sub-harmonic waves can be seen in the spectra of both vertical and horizontal displacements. From these results, stick and slip behaviours due to frictions show large nonlinearities in higher harmonics and sub-harmonics.

## 7. Conclusions

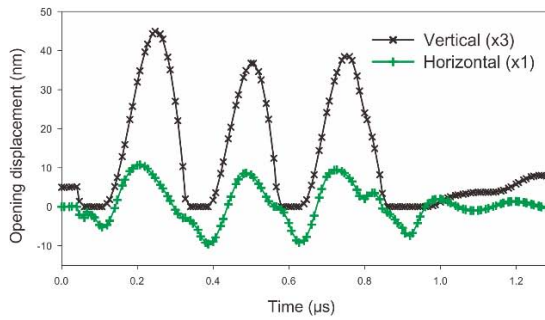
In this paper, the boundary integral equations for bi-material subjected to an incident plane wave were reformulated, and the IRK based CQ-BEM was implemented in the numerical simulation. The interface conditions for debonding areas that consists three phases of separation, stick and slip, were developed for the simulation of nonlinear ultrasonic waves. Numerical results showed that nonlinear ultrasonic waves are generated, largely depending on the contact conditions on the interface, especially, frictional conditions in “stick” and “slip” play an important role to cause nonlinear waves.



(a)

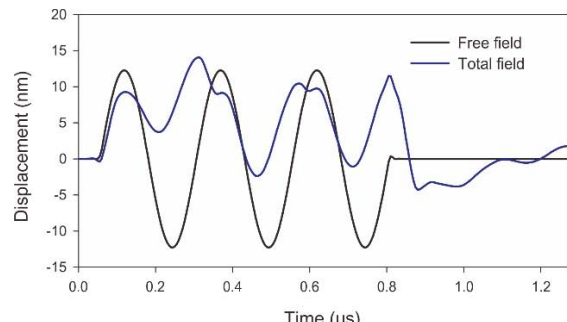


(b)

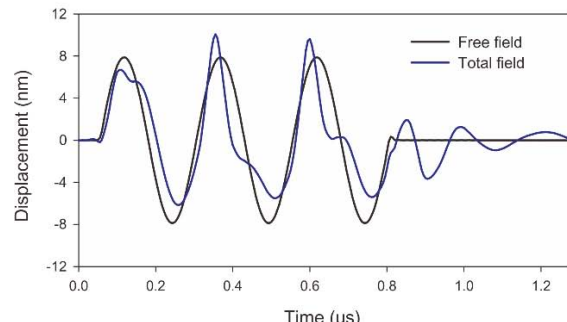


(c)

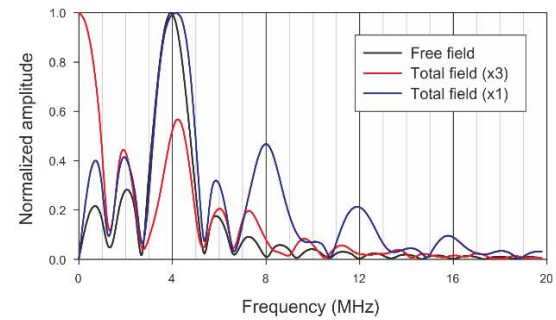
Fig. 6 Time variations of (a) vertical and (b) horizontal displacements at the center points on upper and lower debonding surfaces and (c) vertical and horizontal components of crack opening displacements at the center in the cases of oblique incidence with 30 degrees of sinusoidal P waves with 4MHz frequency.



(a)



(b)



(c)

Fig. 7 Time variations of (a) vertical and (b) horizontal displacements at the point 0.1mm above the center of debonding surface in the cases of oblique incidence with 30 degrees of sinusoidal P waves with 4MHz frequency, and (c) the Fourier spectra.

## REFERENCES

- Brebbia, C.A., Telles, J.C.F., Wrobel C.L. (1984), *Boundary element techniques, Theory and applications in engineering*, Springer, Berlin, Germany
- Lubich, C. and Ostermann A. (1993), "Runge-Kutta methods for parabolic equations and convolution quadrature", *Math. Comp.*, **60**, 105-131.
- Hirose, S., (1994), "2-D scattering by a crack with contact boundary conditions", *Wave Motion*, **19**, 37-49.
- Maruyama, T., Saitoh, T., and Hirose, S. (2012), "Implicit Runge-Kutta based convolution quadrature boundary element method and its application to 3-D scalar wave propagation problems", *JASCOME*, **12**, 91-96 (in Japanese).
- Saitoh, T. and Hirose, S. (2010), "Parallelized fast multipole BEM based on the convolution quadrature method for 3-D wave propagation problems in time-domain", *IOP Conf. Series: Materials Science and Engineering*, **10**, 012242.
- Saitoh, T., Furuta, Y., Hirose, S. and Nakahata, K. (2011), "Simulation of Higher Harmonics on Nonlinear Ultrasonic Testing Using Convolution Quadrature Time-Domain Boundary Element Method in 2-D Elastodynamics", *Journal of Japan Society of Civil Engineers, Ser. A2 (JSCE J. Applied Mech.)*, **67**, 2, pp. I\_161-I\_169 (in Japanese).
- Solodov, I., Doring D. and Busse G. (2011), "New opportunities for NDT using non-linear interaction of elastic waves with defects", *J. Mech. Eng.* **57**, 3, 169-182.